Pergamon

0039-9140(93)E0040-K

Talanta, Vol. 41, No. 5, pp. 747–754, 1994

0039-9140/94 $7.00 + 0.00

MECHANISTIC STUDIES OF CHELATING RESINS USING TWO-PHASE POTENTIOMETRY

NEIL V. JARVIS and JUDITH M. WAGENER*

Department of Process Technology, Atomic Energy Corporation of South Africa Ltd, P.O. Box 582, Pretoria, 0001, South Africa

(*Received* 19 *August* 1993. *Revised* 16 *November* 1993. *Accepted* 22 *November* 1993)

Summary—The elucidation of metal ion binding mechanisms with chelating resins by treating the resin as a collection of monomeric units is an established approach. In this paper, this approach is used to treat data obtained from two-phase potentiometric titrations by the programme ESTA. Apparent protonation and formation constants could be calculated. From these, species distribution plots could be obtained. These, in turn, allowed the calculation of the more familiar distribution ratios. The method was tested on Fe(III) and Nd(III) bonding with the iminodiacetate functionalized resin, Chelex† 100; and Ca(II) bonding to the aminomethylphosphonate functionalized resin, Purolite S940. Good results were obtained indicating the applicability of this method. Comparisons with the literature are made.

In the two decades after the first synthesis of chelating resins in the 1950s, a number of mechanistic studies were performed by treating the resin as a collection of monomeric units. The best studied resin was Chelex 100 (Dowex A-1), a polystyrene-divinylbenzene copolymer functionalized with iminodiacetate groups. Loewenschuss and Schmuckler[1] found that there was a correlation between the apparent formation constants of metal ions with the resin and those of the monomeric analogue, N-benzyliminodiacetate. Other aspects of early mechanistic studies on Chelex 100 are adequately reviewed by Marcus and Kertes.[2] From the late 1960s until the present, most studies with chelating resins have focused on the acquisition of distribution ratio data from batch experiments with little effort going into mechanistic studies. Recently, Högfeldt[3] showed that his three-parameter model could be extended to chelating resins. This was done by using data obtained by Marinsky[4] on Dowex A-1 in the 1960s. Högfeldt commented that the approach of using the monomer to predict titration curves had not up until then been widely used probably because of unwieldiness. The method of data acquisition was no doubt a contributing factor to this unwieldiness, given that each titration point had to be obtained using batch experiments.

Some of these problems may now be overcome by using automatic titrators and sophisticated computer software. Continuous titrations replace batch experiments and the data may be analysed by a program such as ESTA.[5] Satisfactory results may be obtained even though ESTA was designed to calculate formation constants of solution species. It was found that when the program considered that the monomeric units of the chelating resin were in solution, apparent formation constants could be accurately calculated and mechanisms of metal ion bonding could be elucidated. The method was tested on Fe(III) and Nd(III) with Chelex 100 and Ca(II) with Purolite S940, an aminomethylphosphonate functionalized resin often used for water softening.

EXPERIMENTAL

Reagents

Chelex 100 in the sodium form was an analytical grade product obtained from Biorad. The resin was dried overnight in an oven at 90°C, ground to a fine powder and stored in a desiccator. Microanalysis found $\%C = 64.21$, $\%H = 6.63$ and $\%N = 3.63$. Using the calculation method of Loewenschuss and Schmuckler,[1] it was found that exactly one out of every two styrene rings were functionalized and that the

*Part of this work was submitted as an M.Sc. thesis to the University of Pretoria.

†Chelex is a registered trademark of the Biorad Chemical Company.

Table 1. Compositions of experimental solutions for studies with Chelex 100

Cation	Titration	1*M* $NaNO_3$ (*ml*)	Metal ion solution* (*ml*)	Chelex 100 (*g*)	2*M* $NaNO_3$ (*ml*)	0.050*M* HNO_3 in 0.95*M* $NaNO_3$ (*ml*)
H^+	1	40.0		0.050		10.0
	2	43.0		0.040		7.0
	3	40.0		0.060		10.0
Nd(III)	1	30.0	5.0	0.050	5.0	10.0
	2	30.0	5.0	0.040	5.0	10.0
	3	30.0	5.0	0.060	5.0	10.0
Fe(III)	1	35.0	5.0	0.060	5.0	5.0
	2	35.0	5.0	0.080	5.0	5.0
	3	35.0	5.0	0.10	5.0	5.0

*Solutions made up as follows: 0.00756*M* $Nd(NO_3)_3$ in 0.0097*M* HNO_3 and 0.0161*M* $Fe(NO_3)_3$ in 0.050*M* HNO_3.

dried resin contained no water. The molar mass of the monomeric unit could then be calculated to be 397 g/mol.

Purolite S940 in the sodium form, an analytical grade resin, was treated in the same way as Chelex 100. Microanalysis found $\%C = 51.39$, $\%H = 6.00$ and $\%N = 2.27$. Thus, it could be calculated that exactly every third ring was functionalized and that 21.5% by mass of the resin could be attributed to water. The molar mass of the monomeric unit could then be calculated to be 376 g/mol.

All other reagents used were of analytical grade. Metal ion solutions were acidified to prevent hydrolysis and standardized by neutron activation analysis and/or ICP. Standardized sodium hydroxide solutions were obtained by using Merck Titrisol ampoules.

Potentiometry and computing

Titrations were performed by a Metrohm Titroprocessor 670 using a Metrohm 665 dosimat and a Metrohm combined platinum–glass (Ag/AgCl) electrode. The titration solutions were contained in a jacketed vessel through which water at 25 ± 0.1°C was circulated from a Grant W14 thermostatted bath. The compositions of the titration solutions are listed in Tables 1 and 2. These were performed beginning at low and ending at high pH by the addition of 0.050*M* NaOH in 0.95*M* $NaNO_3$. All titration solutions were held at a constant ionic strength of 1.0*M* $NaNO_3$ and vigourously stirred. Nitrogen gas was bubbled through the solutions during the titrations. Under these conditions, it appeared as though equilibrium was attained within a number of minutes (stable emf readings were obtained). A problem often encountered with two-phase titrations is the length of time needed for equilibrium to be reached after each addition of titrant. The presence of two phases also contributes to electrode drift. This was overcome by programming the Titroprocessor not to add titrant until the electrode drift was less than 0.5 mV/min or a time of 10 min had elapsed. Most data points were obtained using the former criterion. The remaining points were given low weights by the program ESTA2A. Data were submitted to ESTA which was loaded on a mainframe computer. The module ESTA0 was used to calculate experimental formation functions ($\bar{Z}$ = the average number of ligands bound per metal ion; $\bar{Z}_H$ = the average number of protons bound per ligand; and the deprotonation function, $\bar{Q}$ = the average number of protons released on complexation per metal ion) values. Where these were insensible, the data points were rejected for refinement. All

Table 2. Compositions of experimental solutions for studies with Purolite S940

Cation	Titration	1*M* $NaNO_3$ (*ml*)	0.0109*M* $Ca(NO_3)_2$ in 0.05*M* HNO_3 (*ml*)	Purolite S940 (*g*)	2*M* $NaNO_3$ (*ml*)	0.050*M* HNO_3 in 0.95*M* $NaNO_3$ (*ml*)
H^+	1	40.0		0.030		10.0
	2	40.0		0.040		7.0
	3	40.0		0.050		10.0
Ca(II)	1	35.0	5.0	0.030	5.0	5.0
	2	35.0	5.0	0.040	5.0	5.0
	3	35.0	5.0	0.050	5.0	5.0

optimization was done using ESTA2A with the data weighted.[6] Apparent pK_a values obtained in the titrations without metal ions were fixed during optimization of metal ion titrations. Hydrolysis constants and pK_w were obtained from Smith an Martell[7] and also held constant. The electrode constant (E_0) was calculated regularly using a strong acid–base titration. Once a model had been obtained, ESTA2A was allowed to refine E_0 resulting in small changes with improved standard deviations for β values and the Hamilton R-factor. Because cross-linking was neglected in the calculation of the molar mass of the monomeric unit, ESTA2A was also allowed to refine the ligand concentrations once models had been found. Similar trends were noticed as for E_0 with the ligand concentration being refined to within a few percent of the calculated value. It should be noted that E_0 and ligand concentrations should not be refined simultaneously as this generally resulted in unacceptably large changes to either one or the other.

RESULTS AND DISCUSSION

Equilibrium modeling

The results of modelling for Chelex 100 and Purolite S940 are found in Tables 3 and 4, respectively. The low standard deviations of the β values and Hamilton R-Factors indicate the applicability of the method. It therefore appears as though ESTA may be led to believe that the monomeric unit (ligand) is in solution whereas in fact the data were obtained from two-phase titrations. Table 5 shows the small degree (generally to within 5%) to which the ligand concentrations were refined. The program was therefore able to correct for cross-linking in this manner. The only anomaly is the first titration for Ca(II) with Purolite S940 where the ligand concentration was slightly increased on refinement. Perhaps this could be attributed to a weighing error.

Calculated and experimental formation and deprotonation curves were all in good agreement indicating that the chosen models were plausible.

Protonation of Chelex 100

The apparent first dissociation constant at 25°C and infinite dilution for the iminodiacetate functional group has been calculated to be 2.92, 2.77 or 2.91[2] by pH and isotope dilution measurements on the sodium–hydrogen exchange. The value of 3.31 obtained here at 1.0*M* ionic strength is therefore in good agreement. Leyden and Underwood[8] stated that the protonation of the weakly acid group led to a pK_2 of 8.57. In this study, three pKs could be discerned with $\log \beta_3$ presumably corresponding to Leyden and Underwood's finding.

Table 3. Apparent protonation and formation constants for Chelex 100*

Cation	Equilibrium†	$\log \beta$	Hamilton R-Factor (R-Limit)	Number of data points
H^+	$H + L = HL$	3.31 ± 0.002		
	$2H + L = H_2L$	5.30 ± 0.007		
	$3H + L = H_3L$	7.46 ± 0.008	0.00886	
			(0.00791)	271
Nd(III)	$M + OH = MOH$	6.0‡		
	$M + 4OH = M(OH)_4$	18.6‡		
	$2M + 2OH = M_2(OH)_2$	14.1‡		
	$M + 2L = ML_2$	5.98 ± 0.004		
	$M + L + OH = MLOH$	12.65 ± 0.003	0.00101	
			(0.00104)	205
Fe(III)	$M + OH = MOH$	11.1‡		
	$M + 2OH = M(OH)_2$	22.0‡		
	$2M + 2OH = M_2(OH)_2$	25.0‡		
	$3M + 4OH = M_3(OH)_4$	50.6‡		
	$M + L = ML$	4.26 ± 0.008		
	$M + L + OH = MLOH$	15.27 ± 0.006	0.00123	
			(0.00098)	275

*All data at 25°C in 1.0*M* $NaNO_3$. pK_w was fixed at 13.79 under these conditions.[7]

†In these equilibria, charges on metal ions, the ligand and complexes have been omitted for simplicity. *L* = deprotonated monomeric unit of Chelex 100, M = metal ion, H = proton and OH = hydroxide ion.

‡Estimated from Ref. 7.

Table 4. Apparent protonation and formation constants for Purolite S940*

Cation	Equilibrium†	log β	Hamilton R-Factor (R-Limit)	Number of data points
H^+	$H + L = HL$	7.51 ± 0.01		
	$H + 2L = HL_2$	10.71 ± 0.03		
	$3H + L = H_3L$	12.08 ± 0.01		
	$3H + 2L = H_3L_2$	20.85 ± 0.02	0.0184 (0.00911)	269
Ca(II)	$M + OH = MOH$	0.8‡		
	$M + 2L + H = ML_2H$	17.96 ± 0.02		
	$M + 2L + OH = ML_2OH$	17.03 ± 0.02		
	$M + 2L + 2OH = ML_2(OH)_2$	21.48 ± 0.01		
	$M + 2L + 3OH = ML_2(OH)_3$	24.52 ± 0.02		
	$M + 3L = ML_3$	17.88 ± 0.01		
	$M + 3L + H = ML_3H$	10.62 ± 0.02		
	$M + 3L + 2H = ML_3H_2$	28.50 ± 0.02		
	$M + 3L + OH = ML_3OH$	23.41 ± 0.02	0.00634 (0.00117)	356

*All data at 25°C in 1.0*M* $NaNO_3$. pK_w was fixed at 13.79 under these conditions.[7]

†In these equilibria, charges on metal ions, the ligand and complexes have been omitted for simplicity. L = deprotonated monomeric unit of Purolite S940, M = metal ion, H = proton and OH = hydroxide ion.

‡Estimated from Ref. 7.

The protonation formation curves (Fig. 1) show no marked inflections indicating that the ligand's deprotonation reactions overlap in the pH region studied. The greater ability of Chelex 100 for complexing metal ions at higher pH values may be understood from a species distribution plot calculated from the protonation constants obtained in which it may be seen that the resin only becomes fully deprotonated above pH = 5.

Nd(III) complexation by Chelex 100

The formation curves (Fig. 2) exhibit back-fanning indicating that hydrolysis becomes important as the titrations proceed. Accordingly, an NdLOH complex is to be found in the model. Species of the type M_2L_3H as proposed by Hering[9] for Yb(III) could not be found for Nd(III). Perhaps the difference in ionic radius between Nd(III) and Yb(III) may account for this. The greater coordination requirements of Nd(III) as compared to Fe(III) is possibly the reason why an ML_2 species is found for the former while only an ML species with the latter. The apparent formation constant for the ML_2 species corresponds closely with that of the ML species for Nd(III) complexation by N-benzyl-iminodiacetate.[7] This contradicts the finding of Loewenschuss and Schmuckler[1] that apparent formation constants for the resin are similar to

Table 5. Comparison between calculated and refined ligand concentrations

Resin	Cation	Titration	Calculated [L] (*M*)	Refined [L] (*M*)	Difference (%)
Chelex 100	H^+	1	0.00252	0.00245	2.8
		2	0.00202	0.00197	2.5
		3	0.00302	0.00292	3.3
	Nd(III)	1	0.00252	0.00239	5.1
		2	0.00202	0.00194	4.0
		3	0.00302	0.00288	4.6
	Fe(III)	1	0.00302	0.00291	3.6
		2	0.00403	0.00388	3.7
		3	0.00504	0.00486	3.6
Purolite S940	H^+	1	0.00213	0.00209	1.9
		2	0.00266	0.00254	4.5
		3	0.00160	0.00157	1.9
	Ca(II)	1	0.00160	0.00164	−2.5
		2	0.00213	0.00212	0.94
		3	0.00266	0.00258	3.0

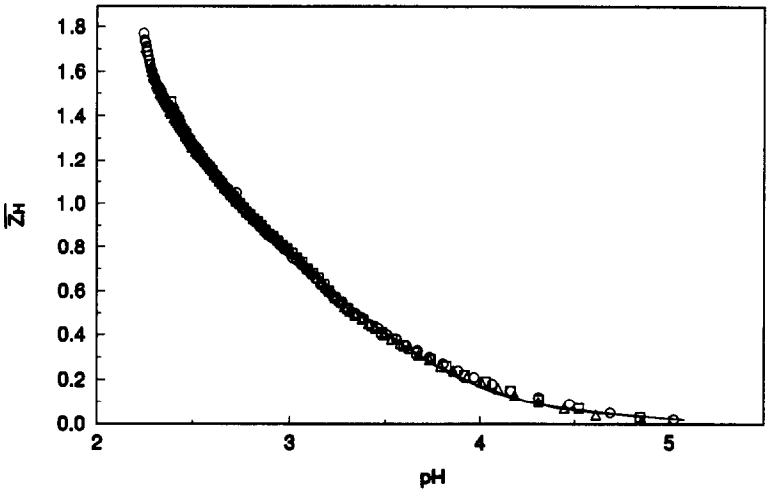

Fig. 1. Experimental (points) and modelled (lines) protonation formation curves for Chelex 100. $\bar{Z}_H$ is the protonation formation function (the average number of protons bound per ligand) and pH is the negative logarithm of the free hydrogen ion ocncentration. The compositions of the solutions are in Table 1. The titrations are represented by (○) titration 1, (△) titration 2 and (□) titration 3. All solutions were at 25°C and 1.0*M* with respect to $NaNO_3$.

the formation constants for the monomeric ligand. Accordingly, a new search was launched to obtain an ML species in the model. This was unsuccessful. The observation that Nd(III) does not follow Loewenschuss and Schmucklers' rule needs further investigation. The good agreement between experimental and calculated deprotonation curves (Fig. 3) lends further credibility to the model.

The species distribution plot shows that Nd(III) is complexed by the resin above pH = 2 with quantitative complexation probably occurring only at about pH = 6. Metal ion hydroysis is suppressed in this range. The $Nd(OH)_3$ species cannot be handled by ESTA. Therefore, a check was made that the solubility product[7] of this species was not exceeded at any stage during the titrations. This was done using free metal ion concentrations calculated at discrete pH values by the program ESTA1 (task SPEC). It was found that the solubility product was not exceeded at any pH value used in modelling.

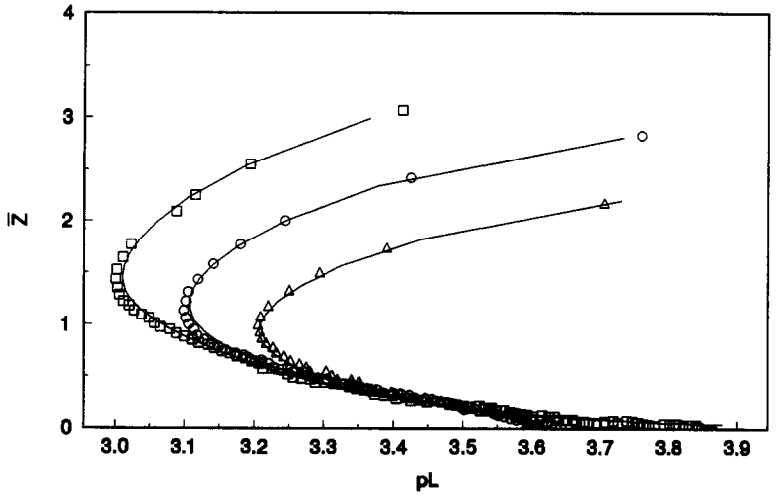

Fig. 2. Experimental (points) and modelled (lines) formation curves for Nd(III) complexation by Chelex 100. $\bar{Z}$ is the formation function (the average number of ligands bound per metal ion) and pL is the negative logarithm of the free ligand concentration. The compositions of the solutions are in Table 1. The titrations are represented by (○) titration 1, (△) titration 2 and (□) titration 3. All solutions were at 25°C and 1.0*M* with respect to $NaNO_3$.

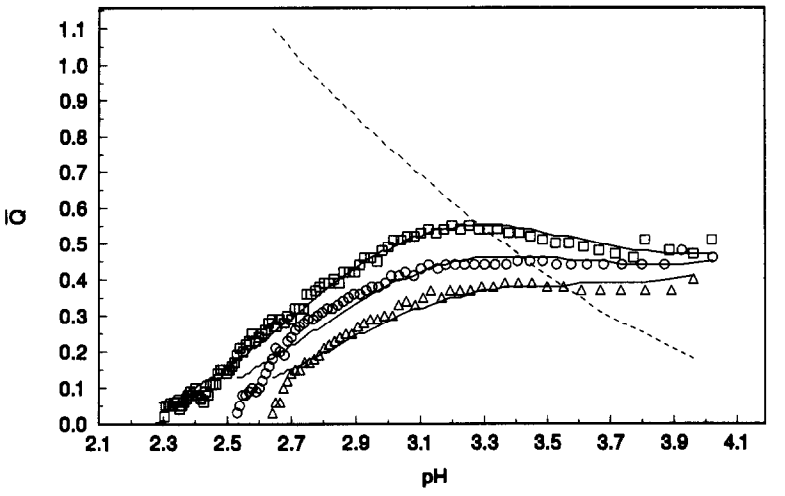

Fig. 3. Experimental (points) and modelled (lines) deprotonation curves for Nd(III) complexation by Chelex 100. $\bar{Q}$ is the deprotonation function (the average number of protons released on complexation per metal ion). The dashed line is the $\bar{n}$ curve where $\bar{n}$ is the deprotonation curve for the ligand in the absence of the metal ion. The compositions of the solutions are in Table 1. The titrations are represented by (○) titration 1, (△) titration 2 and (□) titration 3. All solutions were at 25°C and 1.0*M* with respect to $NaNO_3$.

Fe(III) complexation by Chelex 100

Both formation and deprotonation curves show that at low pH, Fe(III) is already extensively complexed by the resin (Figs 4 and 5). Back-fanning once again points to hydrolysis. The $Fe(OH)_3$ species could not be included and so a similar procedure as for Nd(III) above was followed to ensure that the solubility product was not being exceeded. This was found to be the case between pH 2 and 4. Above pH = 4, metal ion hydrolysis becomes important.

*Protonation of Purolite S*940

Besides the more usual mononuclear species, protonated species involving two repeating units were also found. This points to the program being sensitive to intramolecular hydrogen bonding.

The protonation formation curves (Fig. 6) show a marked inflection at $\bar{Z}_H = 1$ indicating the presence of an HL species. This was indeed found to be the major complex in the pH range of the inflection.

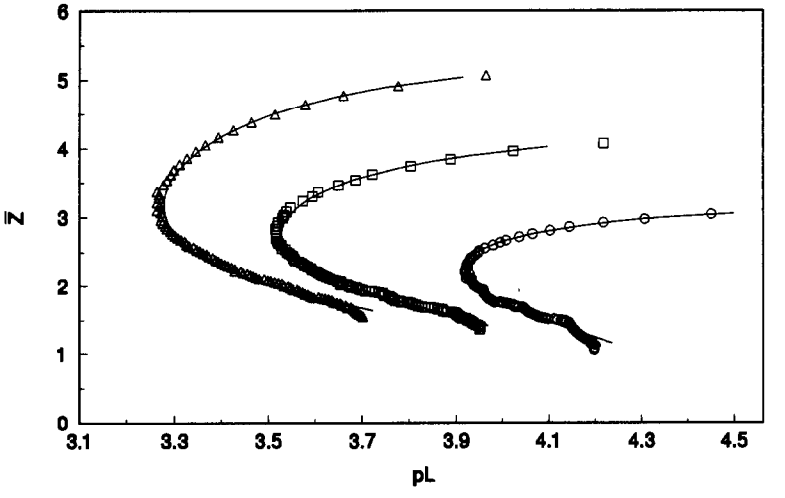

Fig. 4. Experimental (points) and modelled (lines) formation curves for Fe(III) complexation by Chelex 100. The compositions of the solutions are in Table 1. The titrations are represented by (○) titration 1, (□) titration 2 and (△) titration 3. All solutions were at 25°C and 1.0*M* with respect to $NaNO_3$.

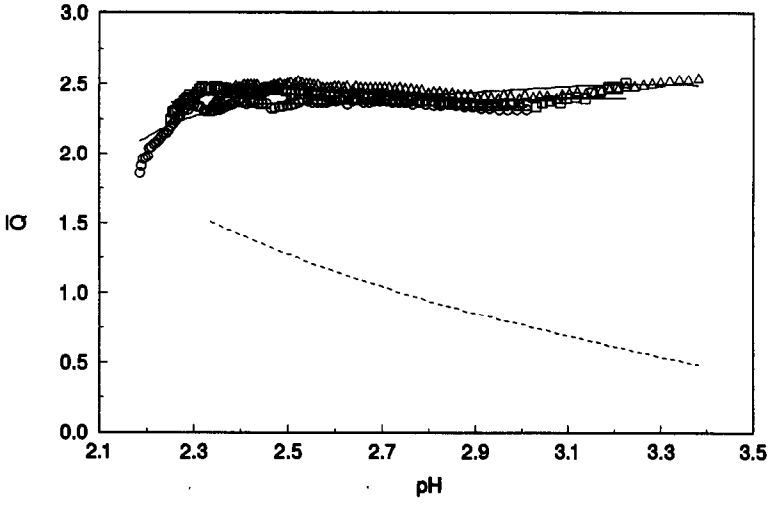

Fig. 5. Experimental (points) and modelled (lines) deprotonation curves for Fe(III) complexation by Chelex 100. The compositions of the solutions are in Table 1. The titrations are represented by (○) titration 1, (□) titration 2 and (△) titration 3. All solutions were at 25°C and 1.0*M* with respect to $NaNO_3$.

Ca(II) complexation by Purolite S940

Formation function curves could not be calculated by ESTA0 or ESTA1 as both are only able to handle protonation constants of species involving one ligand unit. Therefore no information as to model choice could be gleaned from this source. A large number of models were tested with many giving low $\log \beta$ standard deviations and Hamilton R-factors. The best model was chosen according to the closeness of fit of calculated and experimental deprotonation curves (Fig. 7). This criterion is particularly suitable given the convoluted nature of the curves. It was our experience that a number of models, even at low standard deviations and Hamilton R-factors, gave rise to poorly fitting calculated deprotonation curves. The model which fits the curves is therefore particularly plausible.

Calculation of distribution coefficients and separation factors

Distribution coefficients (equivalents metal ion per gram resin/equivalents metal ion per millilitre solution) could be calculated at discrete pH

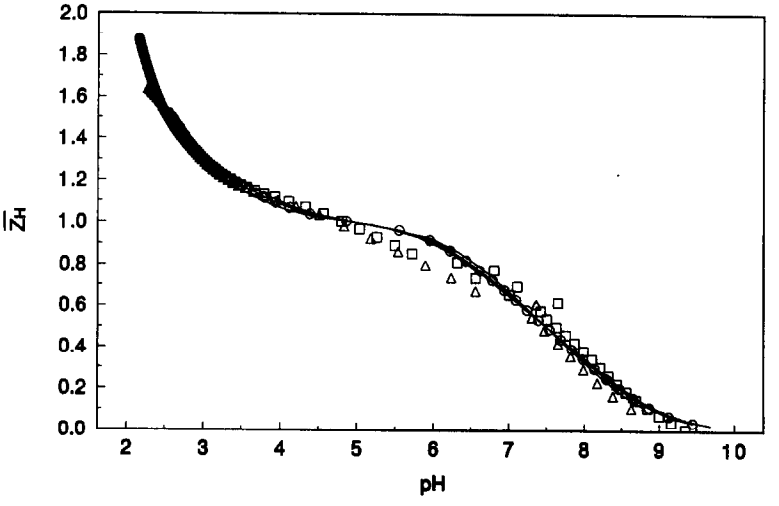

Fig. 6. Experimental (points) and modelled (lines) protonation formation curves for Purolite S940. The compositions of the solutions are in Table 2. The titrations are represented by (○) titration 1, (□) titration 2 and (△) titration 3. All solutions were at 25°C and 1.0*M* with respect to $NaNO_3$.

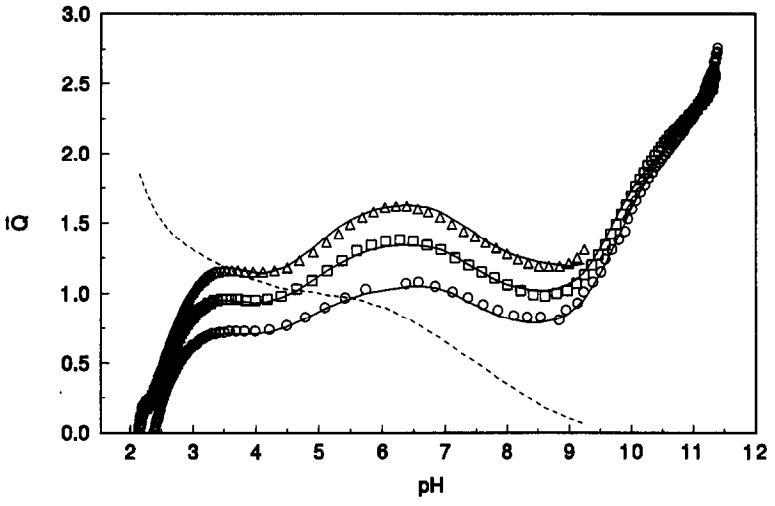

Fig. 7. Experimental (points) and modelled (lines) deprotonation curves for Ca(II) complexation by Purolite S940. The compositions of the solutions are in Table 2. The titrations are represented by (○) titration 1, (□) titration 2 and (△) titration 3. All solutions were at 25°C and 1.0*M* with respect to $NaNO_3$.

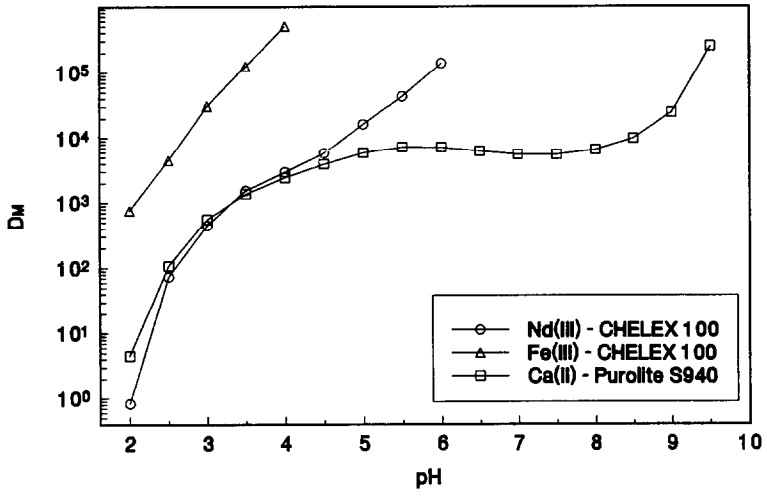

Fig. 8. Distribution coefficients (D_M = equivalents metal ion per gram resin/equivalents metal ion per millilitre solution) versus pH for the metal ions studied.

values from the output of ESTA1 (task SPEC). These are plotted in Fig. 8. It is clear that Fe(III) and Nd(III) may easily be separated using Chelex 100.

Acknowledgement—The authors wish to thank the Atomic Energy Corporation for permission to publish this work.

REFERENCES

1. H. Loewenschuss and G. Schmuckler, *Talanta*, 1964, **11**, 1399,
2. Y. Marcus and A. S. Kertes, *Ion Exchange and Solvent Extraction of Metal Complexes*, p. 349. Wiley-Interscience, New York, 1969.
3. E. Högfeldt, *J. Phys. Chem.*, 1988, **92**, 6475.
4. J. Krasner and J. A. Marinsky, *J. Phys. Chem.*, 1963, **67**, 2559.
5. P. M. May, K. Murray and D. R. Williams, *Talanta*, 1985, **32**, 483.
6. P. M. May and K. Murray, *Talanta*, 1988, **35**, 927.
7. A. E. Martell and R. M. Smith, *Critical Stability Constants*, Vols 1–6. Plenum, New York, 1974–1988.
8. D. E. Leyden and A. L. Underwood, *J. Phys. Chem.*, 1964, **68**, 2093.
9. R. Hering, *J. Inorg. Nucl. Chem.*, 1962, **24**, 1399.